

# Centrifuge modelling of the loading capacity of suction anchors in soft clay: towards multidirectional load.

C.Y. Soriano, L. Thorel, M. Blanc

*Université Gustave Eiffel, Nantes, France,*

*cristian.soriano-camelo@univ-eiffel.fr, luc.thorel@univ-eiffel.fr, matthieu.blanc@univ-eiffel.fr*

**ABSTRACT:** In the framework of the development of solutions for the installation of wind farms in offshore locations, floating wind turbines are an attractive solution to access strong and stable wind conditions. This type of solution faces several challenges, including the mooring and anchoring costs. Anchor sharing is a means to optimize costs for potential wind farms based on floating platforms, as it implies a reduced number of anchors installed, less installation time and a reduced pressure on the supply chain. Recent research efforts on this topic have treated the problem in sandy soil profiles. ShareWind project aims at studying the loading capacity of suction anchors installed in soft clay seabed profiles and subjected to multidirectional loading. This paper introduces the initial development of the project, which involves a series of monotonic unidirectional loading tests conducted at the geotechnical centrifuge of Université Gustave Eiffel in France. The tests consisted of loading three suction anchors installed in kaolin clay, two anchors subjected to lateral load and one anchor to pullout load, to establish a baseline of monotonic loading capacities. Drawing from the insights gained in this inaugural experimental campaign, this paper outlines the proposed experimental setup and loading sequence for transitioning towards multidirectional loading conditions.

## 1 INTRODUCTION

In the context of renewable energies, research efforts are underway to develop anchoring systems for floating wind turbines (Aubeny 2017; Knappet et al. 2015; Randolph 2020). Among the various anchor types (gravity, pile, and plate), new approaches are being explored to optimize the costs and environmental impacts associated with the development of offshore wind farms. One such alternative involves sharing anchors, where multiple mooring lines are connected to a single anchor (Fontana et al. 2018).

ShareWind project aims to leverage the expertise accumulated in the offshore industry regarding suction anchor design considerations and the concept of shared anchors. To this end, a series of centrifuge model tests will be conducted to evaluate the load-bearing capacity of suction caissons subjected to multidirectional loading.

This paper presents the initial stage of the experimental setup development, aimed at determining the lateral load capacity and pull-out capacity under monotonic load of suction anchors installed in kaolin clay. The results of the centrifuge experiment provide data for constructing baseline load envelopes of monotonic loading capacity for suction anchors. Additionally, the insights gained from this initial experimental campaign serve as a foundation for designing the future experimental

setup to apply multidirectional loading to suction anchors.

## 2 MODEL PREPARATION

For the centrifuge experiment, a cylindrical container with an inside diameter of 895 mm and a height of 700 mm was used. The kaolin clay profile was consolidated in four layers, each subjected to different pre-consolidation pressures. As illustrated in Figure 1, Layer 1 at the base of the clay was subjected to a pre-consolidation pressure of 147.4 kPa, Layer 2 was pre-consolidated at 102.3 kPa, Layer 3 at 59.7 kPa, and Layer 4 at 19.5 kPa. Upon the completion of the consolidation of these four layers, a soft clay profile with a thickness of 350 mm was achieved. This procedure was implemented with the aim of modelling a normally consolidated clay profile. The selected pre-consolidation pressures correspond to the effective vertical stress ( $\sigma'_v$ ) at the middle of each layer during the centrifuge test. This methodology was chosen due to the limitations of consolidating clay samples in-flight in the centrifuge.

For the vertical effective stress, a total unit weight of  $\gamma=16.5 \text{ kN/m}^3$  and an effective unit weight of  $\gamma'=6.5 \text{ kN/m}^3$  were employed for the clay. For the estimation of the target vertical effective stresses, a scale factor of  $N=75$  was assumed between the prototype and the model.

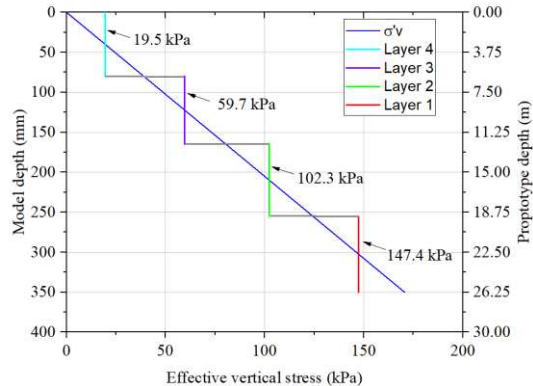


Figure 1. Applied stress for clay consolidation.

Before the installation of the first clay layer, a sand layer with a thickness of 110 mm was placed at the base of the model container. This was designed to facilitate the drainage of water from the clay. A geotextile was positioned on top of the drainage layer to separate the sand and the clay. It is worth mentioning that the sand layer does not influence the geotechnical behavior of the anchors and was used solely for model preparation purposes. Consolidation pressures were applied using a hydraulic piston equipped with a digital control system for pressure regulation. The initial pressure applied to the clay corresponded to the self-weight of the piston, equivalent to 6.9 kPa. Figure 2 depicts a view of the loading system and the installation of one of the clay layers in the model container.

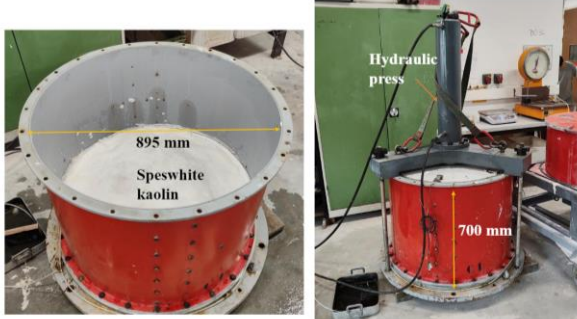


Figure 2. Setup for clay consolidation.

### 3 EXPERIMENTAL SETUP

The experimental setup involved installing three suction anchors to conduct two lateral loading tests and one pullout test. The scale factor between the prototype and the model was  $N=75$ , a value employed in similar experimental setups at the Gustave Eiffel centrifuge laboratory (Cathie et al., 2020). Table 1 summarizes the model and prototype dimensions for the centrifuge test.

The anchors were installed at 1g by manually pushing them into the clay. The installation depth corresponded to the full length of the anchors (200

mm). This process was carried out by opening the top valves of the anchors to let the air inside the caisson flow out (Figure 3).

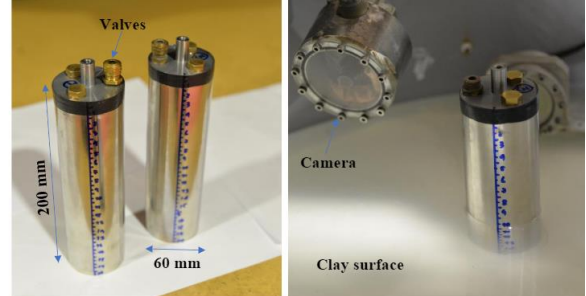


Figure 3. Installation of suction anchors.

In the sequence, a pore pressure transducer (PPT) was carefully pushed throughout the 5 mm diameter opening of the valve. The valve is equipped with internal O-rings that seal the space between the PPT cable and the valve opening. Figure 4 illustrates the installation procedure of a PPT at the top of an anchor.

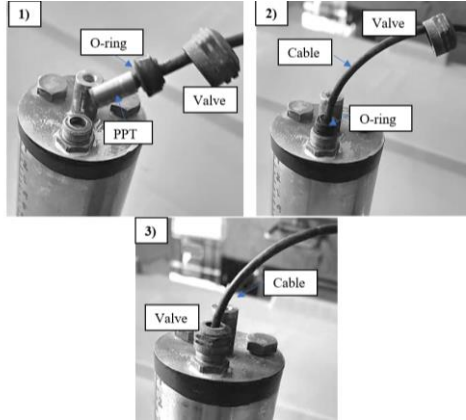


Figure 4. Installation of a PPT.

During the installation of the anchors, some remoulding around the anchor-clay interface may occur. To account for this, the model with the anchors installed was kept in-flight during the centrifuge test for approximately 5 hours (model scale) before the loading tests. This ensured a setup time for the anchors equivalent to 38 months at the prototype scale, thereby guaranteeing a uniform stress field for the loading tests. For reference, Madabhushi (2015) presents a list of the scaling laws between a prototype and a model in centrifuge testing.

After the installation of the suction anchors, a system of gantries and supports was positioned to accommodate a unidirectional electric actuator for applying loads to the anchors. Figure 5 depicts the test setup for the vertical loading (pullout) and lateral loading tests. Figure 6 provides a general view of the centrifuge test setup, including a pulley employed for the lateral loading test, a lighting system, and cameras employed to monitor the loading tests. Both

the cameras and the lights are designed to withstand immersion beneath the water table.

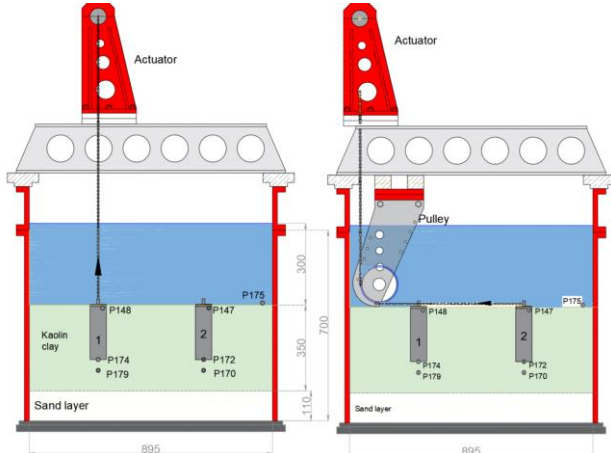


Figure 5. Pullout and lateral load test setup.

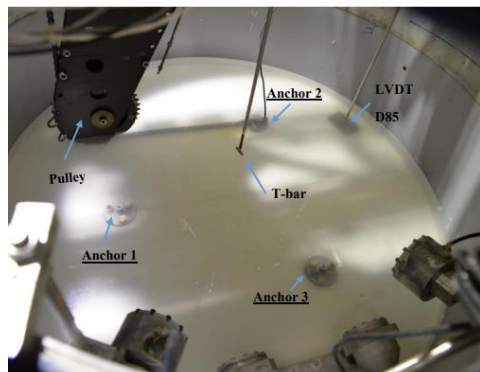


Figure 6. Details of the centrifuge test setup

Table 1. Prototype and model dimensions.

Dimension	Model (1/75)	Prototype
<b>Suction anchor</b>		
Material	Stainless steel	--
D (diameter)	60 mm	4.5 m
L (length)	200 mm	15.0 m
L/D	3.3	3.3
t (wall thickness)	0.41 mm	3.0 cm
D/t	150	150
W (weight)	256.3 g	1.08 MN
W' (buoyant weight)	218.5 g	0.903 MN
<b>Model Container</b>		
Height	700 mm	52.5 m
Height extension	160 mm	12.0 m
Diameter	895 mm	67.1 m
Water table	300 mm	22.5 m
<b>Soil layers</b>		
Clay 4 (Top)	105 mm	7.8 m
Clay 3	79 mm	5.9 m
Clay 2	83 mm	6.2 m
Clay 1 (bottom)	83 mm	6.2 m

### 3.1 Testing sequence

Once placed the model in the centrifuge basket, the centrifuge was accelerated in stages of 10-g until reaching the target test level of 75-g. Upon reaching the testing level, the model was kept in flight for 5 hours to allow the re-consolidation of the clay and the setup of the anchors. Each anchor loading test took one day, resulting in a total of three days to complete the centrifuge test. Table 2 summarizes the testing parameters and the identification of the anchors. As indicated in Table 2, the load ratio of 23 mm/min is consistent with what has been applied in the literature for centrifuge tests in clay under undrained conditions (Chen and Randolph, 2007; Cathie et al., 2020). The larger load ratio of 114 mm/min occurred due to an issue with the actuator control system. Despite this, the results of this experiment are presented in this paper for reference.

Table 2. Identification of loading tests for the suction anchors

Anchor	Load Condition	Loading Rate (model scale)
1	Vertical	23 mm/min
2	Lateral	23 mm/min
3	Lateral	114 mm/min

## 4 TEST RESULTS

For the centrifuge experiment, data acquisition was conducted using the Quantum-X system by HBK. The results were categorized into three groups: (i) force recorded by the load cell of the actuator, (ii) displacements directly retrieved from the actuator, and (iii) pore pressure measurements recorded from three locations. These locations include: (a) one-diameter (1D) below the base of the suction anchors (PPTs P179 and P170 as shown in Figure 4), (b) at the depth of the suction anchor base (PPTs P174 and P172 as shown in Figure 4), and at the top of the anchors (PPTs P148 and P147 as shown in Figure 4)

### 4.1 Pullout test: Anchor 1

The pullout test was conducted by attaching a chain to the top center of the anchor, which was connected to the load actuator. Figure 7 presents the results of the pullout test in prototype scale, illustrating the pullout force and lateral displacements ( $\delta$ ), normalized by the anchor diameter (D). The pore pressure transducer, identified as P174 at the anchor bottom, malfunctioned. Overall, the pullout test yielded a maximum pullout capacity of approximately 5.4 MN, attained at a normalized displacement ( $\delta/D$ ) of around 0.3. Additionally, a

trend in the pore pressures indicated an increase in suction pressures as the pullout displacement increased. This indicates the development of a reverse end bearing mechanism. A preliminary limit equilibrium calculation was conducted in OPTUM G3 (Optum, 2017) based on the undrained shear strength ( $s_u$ ) profile depicted in Figure 10 and simplified in the form of a profile increasing with depth (z):

$$s_u = 1.4 + 0.95z \quad (1)$$

The numerical model yielded a capacity of 5.1 MN, which is consistent with the experimental observations. Figure 8 displays the deformed mesh and the distribution of shear dissipations, illustrating the failure mechanism of the anchor subjected to pullout load.

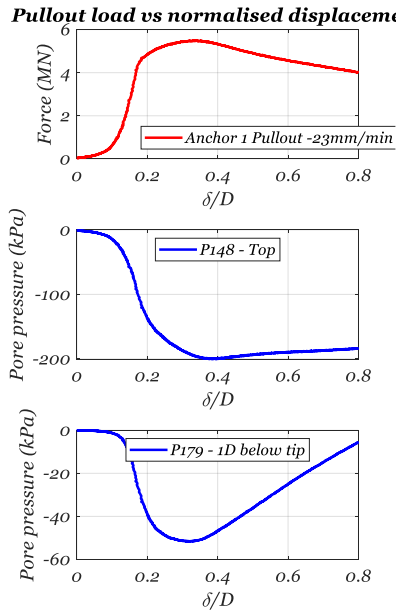


Figure 7. Pullout test results.

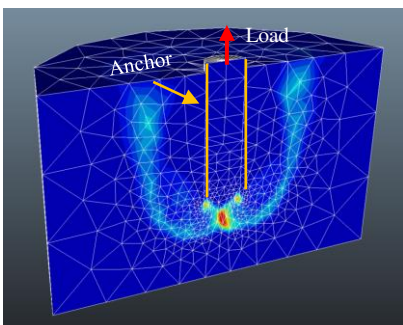


Figure 8. Pullout failure mechanism – Optum G3

## 4.2 Lateral load tests: Anchor 2 & Anchor 3

Figure 9 presents the results of the lateral load tests. For the current test, given the initial state of the project, it was determined the point of application of

the lateral load at the top of the anchors. This condition implies that the anchor's capacity may be higher when applying the lateral load at a deeper location, such as around  $2/3L$  (Randolph and Gourvenec, 2011), where  $L$  represents the anchor's length. The following experiments in the experimental program will include the application of loads at this optimal point of application by the installation of padeyes at the anchors. For the tested condition, it was achieved a lateral load capacity around 1MN for the two anchors tested at two load ratios: 114 mm/min and 23 mm/min. In terms of the pore pressures, it can be seen an increasing trend as the applied lateral displacement progressed reaching a peak value, followed by a drop registered by all the pore pressure transducers.

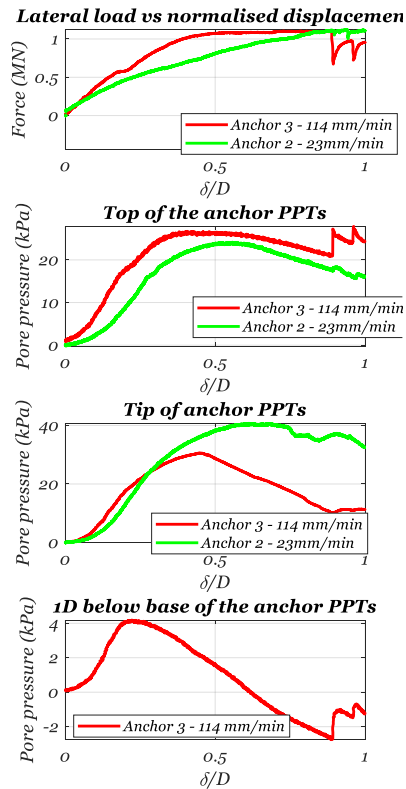


Figure 9. Lateral load test results.

A preliminary limit equilibrium calculation was also conducted in Optum G3 using for this load condition, yielding a capacity of 1.1 MN, which is consistent with the experimental results. The mesh and failure mechanism (shear dissipation) for a lateral load applied at the top of the anchor are depicted in Figure 10. For the lateral load it is evidenced a rotational mechanism at the base and the formation conical wedge from around half of the length of the anchor extending towards the ground surface. The calculations involved the use of a Tresca Basic material for the soil domain, rigid shell elements for the suction caisson and the load applied in the form

of multipliers using as reference a unitary load (1kN) as reference.

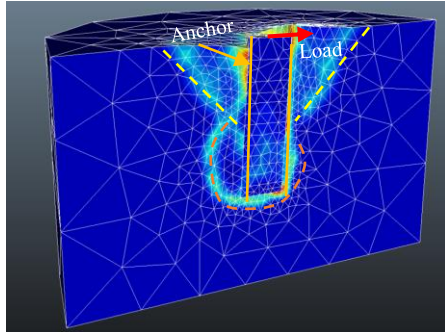


Figure 10. Lateral load failure mechanism – Optum G3

#### 4.3 Strength characterization tests

Figure 11 depicts the strength characterization tests performed on the clay in terms of its undrained shear strength. The T-bar used for these tests has a diameter of 5 mm and a length of 20 mm, resulting in a projected area of  $A=100 \text{ mm}^2$ . The T-bar tests were conducted at a penetration rate of 1 mm/s. To calculate the undrained shear strength profiles, the recorded data from a potentiometer attached to the T-bar actuator and force recordings from a load cell mounted on top of the T-bar were utilized. The T-bar tests were conducted in three different days as one anchor was tested per day. For differentiation, the tests are coded at the end as D1, D2, and D3 for day one, day two and day three of the centrifuge test. The experimental results are compared to a profile calculated using the function derived by Wroth (1984):

$$\frac{s_u}{\sigma'_{vo}} = \left( \frac{s_u}{\sigma'_{vo}} \right)_{nc} OCR^\Lambda \quad (2)$$

Where, the normally consolidated strength ratio  $\left( \frac{s_u}{\sigma'_{vo}} \right)_{nc} = 0.19$ , OCR the over consolidation ratio and the plastic volumetric strain ratio,  $\Lambda = 0.59$ , based on Garnier (2001).

Two cyclic T-bar tests were conducted (labelled CYC in Figure 11) to evaluate the clay's degradation during remoulding. The results of these tests are summarized in Figure 12. Based on the outcomes, the clay sensitivity, defined as the ratio between initial T-bar penetration resistance and post-cyclic penetration resistance, is approximately 2.5. These findings align with cyclic T-bar tests performed on kaolin clay by Zhang et al. (2011).

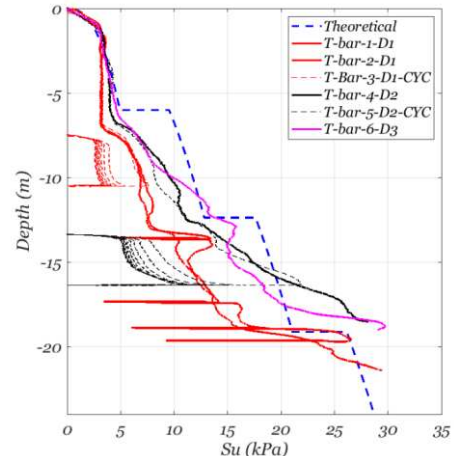


Figure 11. Profiles of undrained shear strength.

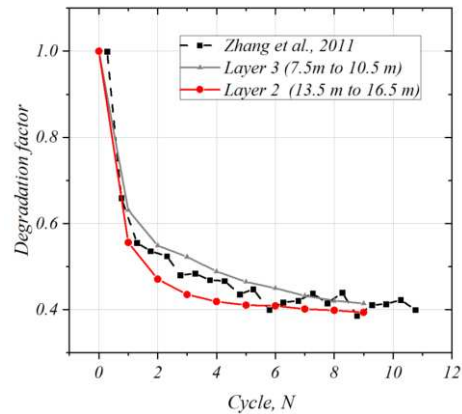


Figure 12. T-bar resistance degradation factor.

## 5 POST-TEST OBSERVATIONS

As part of the experimental setup development, photogrammetry was employed to generate 3D models of the centrifuge experiment after completion of the test. This procedure enables reconstruction of the post-test condition, allowing for the acquisition of additional data on permanent displacements. Detailed information on the workflow developed for generating the virtual models is presented by Soriano et al. (2024). Figure 13 and Figure 14 showcase the generated 3D models uploaded on the Sketchfab platform.

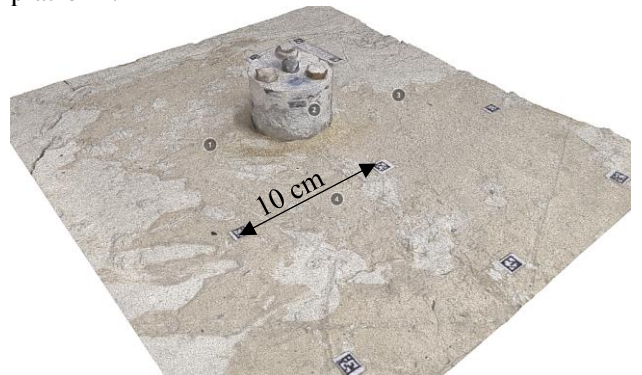


Figure 13. Pullout test anchor. Model available at : <https://skfb.ly/oLHTP>



Figure 14. Lateral test anchor. Model available at :  
<https://skfb.ly/oLAJN>

## 6 CONCLUSIONS

This paper presented the initial stage of the development of an experimental setup to investigate the loading capacity of suction anchors installed in soft clay under multidirectional loading. The following are some of the outcomes of the current study:

- The results of the pullout test showed a maximum pullout capacity of approximately 6 MN, achieved at a normalized displacement of around 0.3. The lateral load tests yielded a lateral load capacity around 1MN for the two anchors tested at two load ratios: 114 mm/min and 23 mm/min.
- The strength characterization tests showed that the undrained shear strength profile can be approximated by the function derived by Wroth (1984). The cyclic T-bar tests showed that the clay sensitivity is around 2.5.
- The photogrammetry results allowed for the reconstruction of the post-test condition and provided additional data in terms of permanent displacements.
- Experimental data was provided in terms of monotonic loading capacity of suction anchors installed in soft clay to be employed in the calibration of numerical models.

## ACKNOWLEDGEMENTS

This project has received funding from the Horizon 2020 research and innovation program of the European Union under the Marie Skłodowska-Curie grant agreement No. 101106921 - "Shared anchors for floating wind turbines."

## REFERENCES

Aubeny, C. (2017). *Geomechanics of Marine Anchors*

(1st. ed.), CRC Press, Boca Raton, Florida, USA (2017). <https://doi.org/10.4324/9781351237376>

Cathie, D., Sassi, K., Blanc, M., Thorel, L., Wallerand, R. (2020) Holding capacity of suction anchors with trench-centrifuge tests results and interpretation. ISFOG 2020, Austin, United States. pp.352-361.

Chen, W., Randolph, M.F. (2004). Uplift capacity of suction caissons under sustained and cyclic loading in soft clay. *Journal of Geotechnical and Geoenvironmental Engineering*. Vol 133, No.11.

Fontana CM, Hallowell ST, Arwade SR, DeGroot, D., Landon, M.E., Aubeny, C., Diaz, B., Myers, A. and Ozmutlu, S. (2018). Multiline anchor force dynamics in floating offshore wind turbines. *Wind Energy*. Vol.21, pp. 1177-1190. <https://doi.org/10.1002/we.2222>

Garnier, J. (2001). Modèles physiques en géotechnique I– evolution des techniques expérimentales et des domaines d’application. *Revue Française de Géotechnique* 97:3–29 (in French). <https://doi.org/10.1051/geotech/2001097003>

Knappet, J., Brown, M., Aldakih, H., Patra, S., O'Loughlin, S., Chow, S., Gaudin, C. and Lieng, J. (2015). A review of anchor technology for floating renewable energy devices and key design considerations *Proceedings of Frontiers in Offshore Geotechnics III*, pp. 887-892, <https://doi.org/10.1201/b18442-127>

Madabhushi, G. (2015). Centrifuge Modelling for Civil Engineers (1st ed.). CRC Press. <https://doi.org/10.1201/9781315272863>

Optum Computational Engineering (2017). OptumG3: Program for Geotechnical Finite Element Analysis. [www.optumce.com](http://www.optumce.com)

Randolph, M. F. (2020). Design of anchoring systems for deep water soft sediments. In *Advances in Offshore Geotechnics: Proceedings of ISOG2019*, pp. 1-28, Springer Singapore. [https://doi.org/10.1007/978-981-15-6832-9\\_1](https://doi.org/10.1007/978-981-15-6832-9_1)

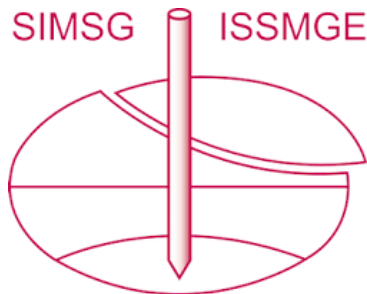
Randolph, M., and Gourvenec, S. (2011). *Offshore Geotechnical Engineering* (1st ed.). CRC Press. <https://doi.org/10.1201/9781315272474>

Soriano, C., Thorel, L., and Blanc, M. (2024). Mobile Photogrammetry for 3D reconstruction of centrifuge experiments in geotechnical engineering. *Journées Nationales de Géotechnique et de Géologie de l'Ingénieur*, Poitiers, France.

Wroth, C.P. (1984). The interpretation of in situ soil tests. *Géotechnique*. Vol 34. No 4. pp 449-489.

Zhang, C., White, D., and Randolph, M. (2011). Centrifuge Modeling of the Cyclic Lateral Response of a Rigid Pile in Soft Clay. *Journal of Geotechnical and Geoenvironmental Engineering*, Vol. 137(7), pp.717-729. [https://doi.org/10.1061/\(ASCE\)GT.1943-5606.0000482](https://doi.org/10.1061/(ASCE)GT.1943-5606.0000482)

# INTERNATIONAL SOCIETY FOR SOIL MECHANICS AND GEOTECHNICAL ENGINEERING



*This paper was downloaded from the Online Library of the International Society for Soil Mechanics and Geotechnical Engineering (ISSMGE). The library is available here:*

<https://www.issmge.org/publications/online-library>

*This is an open-access database that archives thousands of papers published under the Auspices of the ISSMGE and maintained by the Innovation and Development Committee of ISSMGE.*

*The paper was published in the proceedings of the 5th European Conference on Physical Modelling in Geotechnics and was edited by Miguel Angel Cabrera. The conference was held from October 2<sup>nd</sup> to October 4<sup>th</sup> 2024 at Delft, the Netherlands.*

*To see the prologue of the proceedings visit the link below:*

<https://issmge.org/files/ECPMG2024-Prologue.pdf>